Aerospace Science and Technology 109 (2021) 106408

Contents lists available at ScienceDirect

Aerospace Science and Technology

www.elsevier.com/locate/aescte

Understandings of incremental backstepping controller considering measurement delay with model uncertainty

Byoung-Ju Jeon, Min-Guk Seo, Hyo-Sang Shin *, Antonios Tsourdos

Cranfield University, College Road, Cranfield, United Kingdom

ARTICLE INFO

Article history:
Received 5 August 2020
Received in revised form 19 October 2020
Accepted 28 November 2020
Available online 7 December 2020
Communicated by Chaoyong Li

Keywords:
Incremental backstepping control
Measurement delay
Model uncertainty
Closed-loop analysis
Model based algorithm
Sensor based algorithm

ABSTRACT

In this paper, closed loop characteristics with an incremental backstepping (IBKS) controller are investigated with consideration of measurement delays and model uncertainties. To judge absolute stability of the system, a systematic analysis framework is proposed which examines the existence of unstable poles from a derived characteristic equation with high nonlinearity due to the considered measurement delays. One of the key findings from the analysis results is that the system is stable only when a specific relationship between the measurement delays is satisfied and this stability condition is affected by the model uncertainty. Critical understandings about individual and integrated effects of the measurement delays and the model uncertainties to the system are suggested through a comparative study. Verification and validation of the obtained properties from the framework are performed through simulations.

1. Introduction

Backstepping (BKS) control [1] is one of the most widely and successfully applied nonlinear methodologies for a flight control system design [2–10]. One of the issues about the classical backstepping controller is that it is sensitive to model uncertainties, because full model information is explicitly required for its implementation. Note that it is difficult to get an accurate model from a wind tunnel test or an aeroprediction in general. To reduce model dependency of BKS, incremental backstepping (IBKS) controller [11–19] is proposed. Comparing to BKS, IBKS additionally utilizes state derivative and control surface deflection angle measurements which replace required knowledge about a model except control effectiveness information. This algorithm becomes implicit, not totally relying on explicit model information for its implementation.

Since IBKS lies in between sensor based and model based approaches, it is essential to understand the effects of measurement defects such as bias, noise, and delay along with model uncertainties to the closed loop system. There have been some researches investigating closed loop characteristics with IBKS only considering model uncertainties [11–16]. One of the key findings from theoretical analyses in [15] and [16] is that the stability and performance of the system are not affected by any model uncertainties even in control effectiveness information if a control command is calculated, transmitted and reflected fast enough to a real control surface deflection. The limitation of the analyses in previous studies is that measurements are assumed to be ideal, which is impossible in practice. [17] suggested closed loop analysis results with consideration of measurement biases together with model uncertainties. This study indicates that measurement biases only cause additional steady state error. One of the interesting observations is that a model uncertainty in control effectiveness information starts to have an impact to the closed loop system when these measurement biases are additionally considered. To the best of our knowledge, there are no existing researches about IBKS analysis considering measurement delays along with model uncertainties.

Unlike IBKS, there have been some studies [20–22] on incremental nonlinear dynamic inversion (INDI) with consideration of measurement delays. Note that INDI [20–25] is an incremental version of NDI [26], as IBKS to BKS. [20] and [21] only consider delay in the state derivative measurement induced by a filter to attenuate noise which is amplified during state differentiation process. In [22], the induced delay from a filter for noise attenuation together with sensor delays is considered during a flight test. [20–22] briefly mention that measurement delays have critical impacts on the closed loop system with the incremental algorithm. [22] indicates that synchronization between state derivative and control surface deflection angle measurements is essential for a successful flight test with INDI. However, [20–22] just focused on algorithm designs to avoid delay issues without systematic analysis

* Corresponding author.
E-mail address: h.shin@cranfield.ac.uk (H.-S. Shin).

https://doi.org/10.1016/j.ast.2020.106408

or sufficient interpretations on the effects of measurement delays to the system.

Relevant studies with IBKS and INDI urge the needs of detailed analysis on the closed loop system with IBKS considering both measurement delays and model uncertainties. One of the biggest challenges in this analysis is that it is difficult to examine even absolute stability of the system in an analytic way due to exponential terms in a characteristic equation generated from measurement delays. The simplest way to resolve this issue is to approximate the exponential terms with well-known methods like Taylor series expansion, as suggested by previous studies on analysis of delayed systems [27–29]. However, this approximation-based approach has following limitations. First, the approximation holds for small enough delay, but it is difficult to judge whether the existing delay is within an acceptable range for the approximation. Second, derived stability conditions become too sensitive to the order of the approximation and they do not match well with those of the real system as shown in [30].

This paper investigates stability characteristics of the closed loop system with IBKS under measurement delays and model uncertainties through systematic analysis. Considering the limitations of the approximation based approach, the existence of the poles on the right half plane is examined by solving the highly nonlinear characteristic equation of the closed loop system numerically without any approximation. A stability condition for the closed-loop system with IBKS is provided as a relationship between delays on state derivative and control surface deflection angle measurements, and it is shown that this condition is affected by the model uncertainty. A comparative study is suggested which enables critical understandings about individual and integrated effects of measurement delays and model uncertainties to the closed loop system.

The rest of this paper is organized as follows. In section 2, dynamics and derived control algorithm with IBKS are provided as preliminaries. The stability analysis framework is proposed in Section 3 for the closed loop system with IBKS under measurement delays and model uncertainties. Section 4 addresses the analysis results obtained from the proposed framework and the results are verified by carrying out simulations.

2. Preliminaries

For the closed loop analysis in Section 3 and 4, dynamics and control algorithm are suggested in Section 2 as preliminaries. Short period mode dynamics and derived control law with IBKS are given in subsection 2.1 and 2.2 respectively. Note that this paper utilizes IBKS for the inner loop controller design and BKS for the outer loop controller design. As can be seen in [11,13,16,20] and [21], the incremental control algorithm is not generally applied for the outer loop, because more practical ways are available to compensate the required model information without utilizing additional measurements in the outerloop.

2.1. Dynamics

For simplicity of the analysis, this paper considers short period mode dynamics (1) in [31]. Note that the short period mode is of paramount importance in the flight control design because one of the main purposes of a stability augmentation system (SAS) for an aircraft is to enhance this short period mode characteristics.

$$\begin{aligned}\dot{\alpha} &= Z_\alpha^*(M,\alpha)\,\alpha + q + Z_\delta^*(M,\alpha)\,\delta \\ \dot{q} &= M_\alpha^*(M,\alpha)\,\alpha + M_q^*(M,\alpha)\,q + M_\delta^*(M,\alpha)\,\delta\end{aligned}$$

where

$$\begin{aligned}Z_\alpha^*(M,\alpha) &= \frac{\bar{q}S}{m}C_{Z_\alpha}(M,\alpha)\frac{1}{U_0} \\ Z_\delta^*(M,\alpha) &= \frac{\bar{q}S}{m}C_{Z_\delta}(M,\alpha)\frac{1}{U_0} \\ M_\alpha^*(M,\alpha) &= \frac{\bar{q}S\bar{c}}{I_y}C_{M_\alpha}(M,\alpha) \\ &\quad + \frac{\bar{q}S\bar{c}^2}{2I_yU_0}C_{M_{\dot{\alpha}}}(M,\alpha)\frac{\bar{q}S}{m}C_{Z_\alpha}(M,\alpha)\frac{1}{U_0} \\ M_q^*(M,\alpha) &= \frac{\bar{q}S\bar{c}^2}{2I_yU_0}C_{M_q}(M,\alpha) + \frac{\bar{q}S\bar{c}^2}{2I_yU_0}C_{M_{\dot{\alpha}}}(M,\alpha) \\ M_\delta^*(M,\alpha) &= \frac{\bar{q}S\bar{c}}{I_y}C_{M_\delta}(M,\alpha) \\ &\quad + \frac{\bar{q}S\bar{c}^2}{2I_y{U_0}^2}C_{M_{\dot{\alpha}}}(M,\alpha)\frac{\bar{q}S}{m}C_{Z_\delta}(M,\alpha)\end{aligned} \tag{1}$$

State variables α and q denote for an angle of attack and a pitch rate. Control input δ indicates a deflection angle of an elevator. $\bar{q}$, U_0 and M are dynamic pressure, constant velocity and Mach number of an aircraft. For notational convenience, aerodynamic derivatives which are given as functions of M and α will be represented in shorthand form as Z_α^*, Z_δ^*, M_α^*, M_q^* and M_δ^*. $C_{(\cdot)}$ indicates dimensionless aerodynamic coefficients. S, $\bar{c}$, m and I_y denote reference area, reference length, mass and moment of inertia in y-axis of an aircraft, respectively. Dynamics (1) describes a nonlinear system which can be expressed as a parameterized linear system where parameters vary with state variables.

Since IBKS is based on the backstepping algorithm which requires that dynamics should be in strict feedback form, a fin surface is assumed to be a pure moment generator. Note that this assumption is a reasonable for most of aircraft, often made in flight controller design, since C_{Z_δ} is generally small enough to be neglected [31].

$$\begin{aligned}\dot{\alpha} &= Z_\alpha^*\alpha + q \\ \dot{q} &= M_\alpha^*\alpha + M_q^*q + M_\delta^*\delta\end{aligned} \tag{2}$$

For the inner-loop control algorithm design with IBKS, q dynamics in (2) is modified as (3), under the assumption that the states α, q and the control input δ can be represented as combinations of reference points $(\cdot)_0$ and perturbations $\Delta(\cdot)$ around them. This is valid assumption especially with a sufficiently high sampling rate.

$$\begin{aligned}\dot{q} &= M_\alpha^*(\alpha_0+\Delta\alpha) + M_q^*(q_0+\Delta q) + M_\delta^*(\delta_0+\Delta\delta) \\ &= \dot{q}_0 + M_\alpha^*\Delta\alpha + M_q^*\Delta q + M_\delta^*\Delta\delta\end{aligned} \tag{3}$$

As described in [11,16,20,23] and [24], the increments of states, $\Delta\alpha$ and Δq, have much less effects on q dynamics than the increments of control input, $\Delta\delta$. This results in the incremental dynamics (4) for the inner loop control system design with IBKS, which is obtained by neglecting $\Delta\alpha$ and Δq in (3).

$$\dot{q} \simeq \dot{q}_0 + M_\delta^*\Delta\delta \tag{4}$$

The final form of dynamics for the controller design is provided as (5).

$$\begin{aligned}\dot{\alpha} &= Z_\alpha^*\alpha + q \\ \dot{q} &= \dot{q}_0 + M_\delta^*\Delta\delta\end{aligned} \tag{5}$$

State errors are defined as (6).

$$z_1 = \alpha - \alpha_c$$
$$z_2 = q - q_c \tag{6}$$

where subscript c indicates a command.

2.2. Derivation of control law

Under the Lyapunov theory, a control command which achieves asymptotic stability of the system is derived from 2 cascaded designing steps as follows.

First, for the outer loop controller design with BKS, Lyapunov function candidate V_1 considering only z_1 is selected as

$$V_1 = \frac{1}{2} z_1^2 \tag{7}$$

which is positive definite except $z_1 = 0$.

The derivative of V_1 is obtained as

$$\begin{aligned} \dot{V}_1 &= z_1 \dot{z}_1 \\ &= z_1 \left(Z_\alpha^* \alpha + q - \dot{\alpha}_c \right) \end{aligned} \tag{8}$$

In order to satisfy the Lyapunov stability condition, a pseudo-command q_c is designed as

$$q_c = -C_1 z_1 - Z_\alpha^* \alpha + \dot{\alpha}_c \tag{9}$$

which makes negative definite $\dot{V}_1 = -C_1 z_1^2$ except $z_1 = 0$ with a positive design parameter C_1. The state of the fast dynamics, q, is regarded as a control input for the slow dynamics.

Second, for the inner loop controller design with IBKS, Lyapunov function candidate V_2 considering both z_1 and z_2 is defined as

$$V_2 = \frac{1}{2} z_1^2 + \frac{1}{2} z_2^2 \tag{10}$$

which is positive definite except $z_1 = 0$ and $z_2 = 0$.

The derivative of V_2 can be calculated as (11), by utilizing the incremental dynamics of q in (4).

$$\begin{aligned} \dot{V}_2 &= z_1 \dot{z}_1 + z_2 \dot{z}_2 \\ &= z_1 \left(Z_\alpha^* \alpha + q - \dot{\alpha}_c \right) + z_2 \left(\dot{q}_0 + M_\delta^* \Delta\delta - \dot{q}_c \right) \end{aligned} \tag{11}$$

From the pseudo-command (9), $\dot{V}_2$ becomes

$$\dot{V}_2 = z_1 \left(-C_1 z_1 + z_2 \right) + z_2 \left(\dot{q}_0 + M_\delta^* \Delta\delta - \dot{q}_c \right) \tag{12}$$

To satisfy Lyapunov stability condition, $\Delta\delta$ is designed as

$$\Delta\delta = \frac{1}{M_\delta} \left(-C_2 z_2 - z_1 - \dot{q}_0 + \dot{q}_c \right) \tag{13}$$

which makes negative definite $\dot{V}_2 = -C_1 z_1^2 - C_2 z_2^2$ except $z_1 = 0$ and $z_2 = 0$ with positive design parameters C_1 and C_2.

The final form of the derived control algorithm can be suggested as follows.

$$\begin{aligned} q_c &= -C_1 z_1 - \hat{Z}_\alpha^* \alpha + \dot{\alpha}_c \\ \delta &= \delta_0 + \Delta\delta \\ &= \frac{1}{\hat{M}_\delta^*} \left(-C_2 z_2 - z_1 - \dot{q}_0 + \dot{q}_c \right) + \delta_0 \end{aligned} \tag{14}$$

Note that aerodynamic derivatives estimates $\hat{(\cdot)}$ are utilized in (14) instead of real Z_α^* and M_δ^*, because only estimated values for the model information are available in controller design phase. The pseudo-command q_c makes the angle of attack α converge to its desired value α_c, and q achieves q_c by the designed control input δ. Comparing to a control command with pure BKS, explicit utilization of $\hat{M}_\alpha^*$ and $\hat{M}_q^*$ information is not required, since $\Delta\alpha$ and Δq are neglected in q dynamics (4) for the inner loop control algorithm design with IBKS. This implies that model dependency is reduced because $\hat{Z}_\alpha^*$ and $\hat{M}_\delta^*$ are only required for implementation of the algorithm. Instead, measurements about state derivative and control input in the inner loop, $\dot{q}_0$ and δ_0, are additionally required to implement the control algorithm with IBKS.

A flight controller is designed to accomplish asymptotic stability under Lyapunov framework, assuming that there are no measurement defects like delays and model uncertainties. The effects of measurement delays and model uncertainties, which can make aimed performance and stability characteristics in this design phase difficult to be achieved, will be investigated in the closed loop analysis.

3. Stability analysis framework under measurement delays

Section 3 suggests the closed loop analysis framework for the system with IBKS under measurement delays and model uncertainties. Comparing to classical BKS, state derivative and control surface deflection angle measurements are additionally utilized and consequently, model information about control effectiveness is only required for IBKS implementation. Hence, delays $\tau_{\dot{q}}$ and τ_δ on $\dot{q}_0$ and δ_0 measurements together with the model uncertainty $\Delta_{M_\delta^*}$ on $\hat{M}_\delta^*$ are mainly considered in the closed loop analysis. Note that the measurement delays in this paper are defined as final delays on the measurements for control command calculation, including delays from sensors, communication links, and processors with estimation algorithms. $\hat{M}_\delta^*$ is assumed to have the same sign with M_δ^*.

The first step for the stability analysis framework is to derive the transfer function of the closed loop system with IBKS considering $\tau_{\dot{q}}$ and τ_δ along with $\Delta_{M_\delta^*}$, resulting in (15).

$$\frac{\alpha(s)}{\alpha_c(s)} = \frac{\frac{M_\delta^*}{\hat{M}_\delta^*}(C_1 C_2 + 1)}{\phi_1(s) s^2 + \phi_2(s) s + \phi_3(s)}$$

where

$$\begin{aligned} \phi_1(s) &= 1 - e^{-\tau_\delta s} + \frac{M_\delta^*}{\hat{M}_\delta^*} e^{-\tau_{\dot{q}} s} \\ \phi_2(s) &= -(Z_\alpha^* + M_q^*)(1 - e^{-\tau_\delta s}) \\ &\quad + \frac{M_\delta^*}{\hat{M}_\delta^*}(C_1 + C_2 + Z_\alpha^* - Z_\alpha^* e^{-\tau_{\dot{q}} s}) \\ \phi_3(s) &= (Z_\alpha^* M_q^* - M_\alpha^*)(1 - e^{-\tau_\delta s}) \\ &\quad + \frac{M_\delta^*}{\hat{M}_\delta^*}(C_1 C_2 + 1) \end{aligned} \tag{15}$$

A detailed derivation of the transfer function (15) under the piecewise approach [32] is addressed in Appendix A.

The stability of the closed loop system can be examined by searching unstable poles from its characteristic equation in (15). The biggest challenge to obtain poles is that there exist exponential functions from the considered measurement delays. If the exponential functions are approximated as in [27–30], it is difficult to figure out the feasible range of delay for the valid approximation. In addition, [30] addresses that the stability characteristics obtained with Taylor series expansion can be highly sensitive to the order of the approximation. The proposed analysis framework in this paper is based on a numerical approach without approximation, which will be shown in the rest of the steps.

The second step is to reformulate the characteristic equation for numerical pole search. By substituting $s = a + bi$ $(a, b \in \mathbb{R})$ and applying Euler's formula, ϕ_1, ϕ_2 and ϕ_3 in (15) can be rewritten as (16).

$$\begin{aligned}
\phi_1 &= (1 - x_\delta + \Omega x_{\dot{q}}) + i(y_\delta - \Omega y_{\dot{q}}) \\
\phi_2 &= \left\{-(Z^*_\alpha + M^*_q)(1 - x_\delta) + \Omega(C_1 + C_2 + Z^*_\alpha - Z^*_\alpha x_{\dot{q}})\right\} \\
&\quad + i\left\{-(Z^*_\alpha + M^*_q) y_\delta + \Omega Z^*_\alpha y_{\dot{q}}\right\} \\
\phi_3 &= \left\{(Z^*_\alpha M^*_q - M^*_\alpha)(1 - x_\delta) + \Omega(C_1 C_2 + 1)\right\} \\
&\quad + i(Z^*_\alpha M^*_q - M^*_\alpha) y_\delta
\end{aligned} \tag{16}$$

where

$$x_\delta = e^{-\tau_\delta a} cos(\tau_\delta b) \qquad x_{\dot{q}} = e^{-\tau_{\dot{q}} a} cos(\tau_{\dot{q}} b)$$

$$y_\delta = e^{-\tau_\delta a} sin(\tau_\delta b) \qquad y_{\dot{q}} = e^{-\tau_{\dot{q}} a} sin(\tau_{\dot{q}} b) \qquad \Omega = \frac{M^*_\delta}{\hat{M}^*_\delta}$$

From (16) with $s = a + bi$ $(a, b \in \mathbb{R})$, the characteristic equation $\phi_1 s^2 + \phi_2 s + \phi_3 = 0$ can be re-arranged as (17).

$$\phi_1 s^2 + \phi_2 s + \phi_3 = Re(a, b) + Im(a, b) i = 0$$

where

$$\begin{aligned}
Re(a,b) &= (a^2 - b^2)\left[1 - \left\{e^{-\tau_\delta a} cos(\tau_\delta b) - \Omega e^{-\tau_{\dot{q}} a} cos(\tau_{\dot{q}} b)\right\}\right] \\
&\quad - 2ab\left\{e^{-\tau_\delta a} sin(\tau_\delta b) - \Omega e^{-\tau_{\dot{q}} a} sin(\tau_{\dot{q}} b)\right\} \\
&\quad + a\left[-(Z^*_\alpha + M^*_q) + \Omega(C_1 + C_2 + Z^*_\alpha) + M^*_q e^{-\tau_\delta a} cos(\tau_\delta b)\right. \\
&\quad \left. + Z^*_\alpha\left\{e^{-\tau_\delta a} cos(\tau_\delta b) - \Omega e^{-\tau_{\dot{q}} a} cos(\tau_{\dot{q}} b)\right\}\right] \\
&\quad + b\left[M^*_q e^{-\tau_\delta a} sin(\tau_\delta b)\right. \\
&\quad \left. + Z^*_\alpha\left\{e^{-\tau_\delta a} sin(\tau_\delta b) - \Omega e^{-\tau_{\dot{q}} a} sin(\tau_{\dot{q}} b)\right\}\right] \\
&\quad + \left\{(Z^*_\alpha M^*_q - M^*_\alpha)(1 - e^{-\tau_\delta a} cos(\tau_\delta b)) + \Omega(C_1 C_2 + 1)\right\} \\
Im(a,b) &= (a^2 - b^2)\left\{e^{-\tau_\delta a} sin(\tau_\delta b) - \Omega e^{-\tau_{\dot{q}} a} sin(\tau_{\dot{q}} b)\right\} \\
&\quad + 2ab\left[1 - \left\{e^{-\tau_\delta a} cos(\tau_\delta b) - \Omega e^{-\tau_{\dot{q}} a} cos(\tau_{\dot{q}} b)\right\}\right] \\
&\quad - a\left[M^*_q e^{-\tau_\delta a} sin(\tau_\delta b)\right. \\
&\quad \left. + Z^*_\alpha\left\{e^{-\tau_\delta a} sin(\tau_\delta b) - \Omega e^{-\tau_{\dot{q}} a} sin(\tau_{\dot{q}} b)\right\}\right] \\
&\quad + b\left[-(Z^*_\alpha + M^*_q) + \Omega(C_1 + C_2 + Z^*_\alpha) + M^*_q e^{-\tau_\delta a} cos(\tau_\delta b)\right. \\
&\quad \left. + Z^*_\alpha\left\{e^{-\tau_\delta a} cos(\tau_\delta b) - \Omega e^{-\tau_{\dot{q}} a} cos(\tau_{\dot{q}} b)\right\}\right] \\
&\quad + (Z^*_\alpha M^*_q - M^*_\alpha) e^{-\tau_\delta a} sin(\tau_\delta b)
\end{aligned} \tag{17}$$

The last step is to find poles by searching a and b which make both $Re(a, b) = 0$ and $Im(a, b) = 0$ in (17). This is performed by solving the system of these nonlinear equations with a widely known and utilized numerical method [33]. The closed-loop system with IBKS is unstable if there exist at least one solution with $a > 0$.

4. Stability analysis results under measurement delays

Closed loop stability analysis results under measurement delays along with model uncertainties are presented in Section 4, which are obtained by applying the numerical framework in Section 3. Simulations are performed for verification and validation of the identified properties from the framework. As illustrative examples, four different types of aircraft models are considered for analysis and simulation, and their aerodynamic derivatives at certain flight conditions [34] are provided in Table B.1 in Appendix B. The design parameters C_1 and C_2 for the control algorithm are set to be 1.5 respectively. An extensive range of $\tau_{\dot{q}}$ and τ_δ together with $\Delta_{M^*_\delta}$ is introduced to obtain critical insights about the effects of measurement delays along with a model uncertainty on the system. Note that considering the page limit, this paper shows some parts of the results that are representative. The presented cases are with $\tau_{\dot{q}}$ and τ_δ from $0s$ to $0.1s$ with $0.01s$ increment and from $0.1s$ to $0.2s$ with $0.02s$ increment (i.e. $[\{0s : 0.01s : 0.1s\} \cup \{0.1s : 0.02s : 0.2s\}]$) along with $\Delta_{M^*_\delta} = [-50\%, -35\%, -20\%, 0\%, 25\%, 100\%, 200\%, 300\%]$. Initial values for the state variables α and q, and the α-command α_c, are set to be $0°$, $0°/s$ and $1.5°$ respectively.

Table 1
k_{max} for each $\Delta_{\hat{M}^*_\delta}$.

$\Delta_{\hat{M}^*_\delta}$	k_{max}			
	Airplane A	Airplane B	Airplane C	Airplane D
-0.5	0	0	0	0
-0.35	1	1	1	1
-0.2	1	1	1	1
0	1	1	1	1
0.25	2	2	2	2
1	3	3	3	3
2	5	5	5	4
3	6	6	6	5

$\tau_{\dot{q}}$ and τ_δ cases examined to be stable by the framework are illustrated for each $\Delta_{M^*_\delta}$ in Fig. 1. Note that the markers ○, □, ○ and □ in Fig. 1 denote the framework results of aircraft A, B, C and D, respectively. Fig. 1 shows that the closed loop system is stable if $\tau_{\dot{q}} = k\tau_\delta$ and the non-negative k has an upper bound k_{max} which varies with $\Delta_{\hat{M}^*_\delta}$. k_{max} values in Fig. 1 are summarized as Table 1 which provides following observations. For $\Delta_{\hat{M}^*_\delta} = 0$, k_{max} is 1, indicating the system becomes stable when there is no delay on $\dot{q}_0$ measurement (i.e. $\tau_{\dot{q}} = 0$) or when the additional measurements $\dot{q}_0$ and δ_0 are synchronized with the same amount of delay (i.e. $\tau_{\dot{q}} = \tau_\delta$). If $\hat{M}^*_\delta$ is under-estimated (i.e. $\Delta_{\hat{M}^*_\delta} < 0$), k_{max} gets smaller, resulting in reduced number of stable points. On contrary, if $\hat{M}^*_\delta$ is over-estimated (i.e. $\Delta_{\hat{M}^*_\delta} > 0$), k_{max} becomes larger, resulting in increased number of stable points.

The simulation results appear to coincide with the framework results, as can be seen in Fig. 1. Note that the simulation results are given with markers ●, ■, ● and ■ for each aircraft A, B, C and D in Fig. 1. For some representative cases with Aircraft A, time responses are presented in Fig. 2. It is shown in Fig. 2 that the closed-loop system is unstable if $\tau_{\dot{q}}$ and τ_δ do not satisfy $\tau_{\dot{q}} = k\tau_\delta$ $(k \le k_{max})$ even with small deviation.

For better understandings on stability and robustness of the closed loop systems, gain margins under $\tau_{\dot{q}}$ and τ_δ together with $\Delta_{\hat{M}^*_\delta}$ are examined through simulations. For illustrative purpose, a part of results with Aircraft A under $\tau_\delta = \{0s : 0.01s : 0.05s\}$ is given as Fig. 3, but the trend of all results is the same. Fig. 3 indicates that the gain margin increases as $\Delta_{\hat{M}^*_\delta}$ increases under the same $\tau_{\dot{q}}$ and τ_δ. For the same $\Delta_{\hat{M}^*_\delta}$, the gain margin decreases when k approaches to its upper bound k_{max}.

The important findings from the framework results can be summarized as Observation 4.1 and 4.2.

Observation 4.1 *(Stability condition with $\tau_{\dot{q}}$ and τ_δ).* The system with IBKS is stable only when $\tau_{\dot{q}} = k\tau_\delta$ with a non-negative integer k which has an upper bound k_{max}. Otherwise, the closed loop system becomes unstable.

Observation 4.2 *(Effect of $\Delta_{\hat{M}^*_\delta}$ to stability condition).* k_{max} becomes smaller as the model uncertainty on control effectiveness information $\Delta_{\hat{M}^*_\delta}$ decreases.

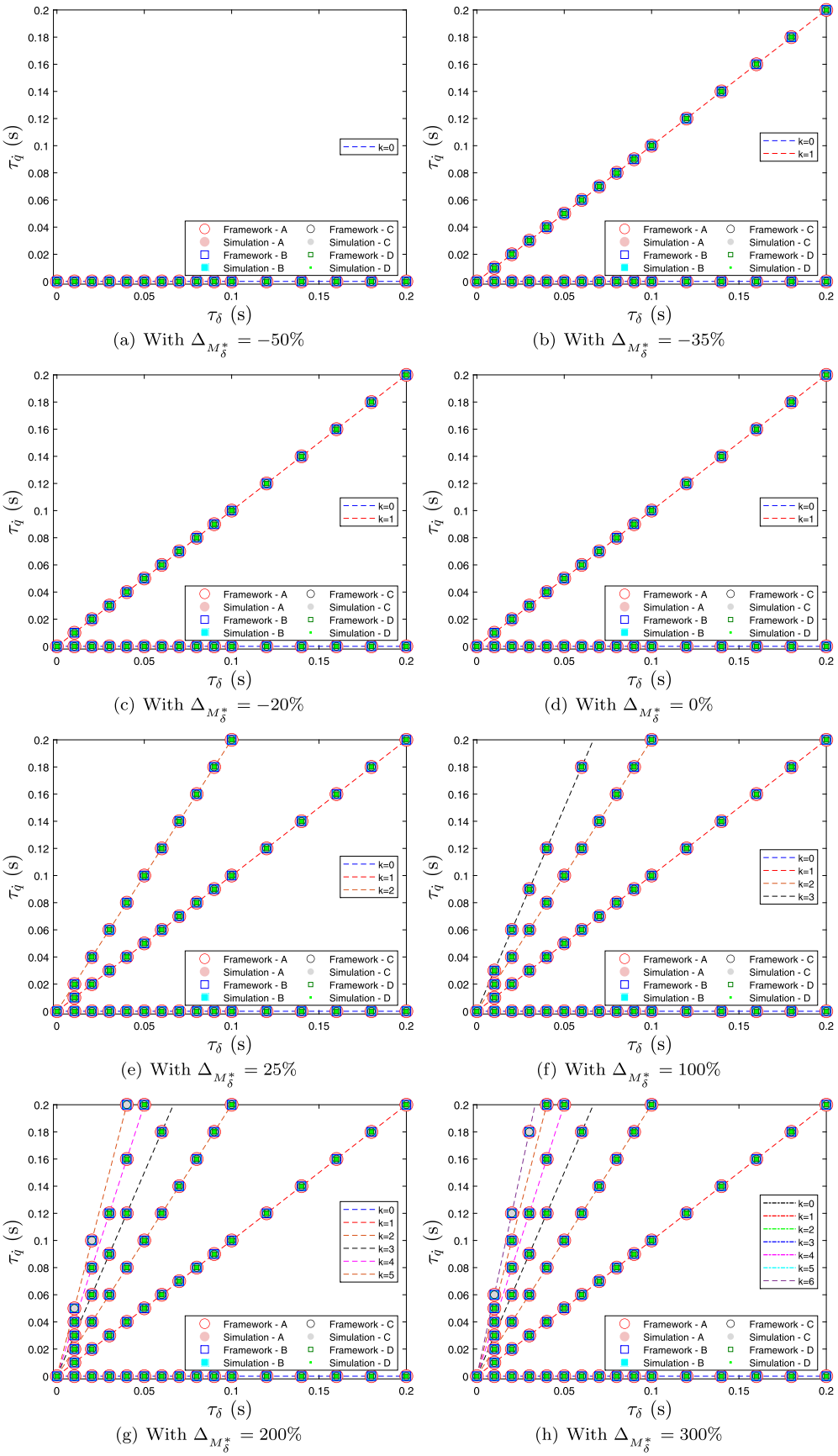

(a) With $\Delta_{M_\delta^*} = -50\%$ (b) With $\Delta_{M_\delta^*} = -35\%$

(c) With $\Delta_{M_\delta^*} = -20\%$ (d) With $\Delta_{M_\delta^*} = 0\%$

(e) With $\Delta_{M_\delta^*} = 25\%$ (f) With $\Delta_{M_\delta^*} = 100\%$

(g) With $\Delta_{M_\delta^*} = 200\%$ (h) With $\Delta_{M_\delta^*} = 300\%$

Fig. 1. Relationships between $\tau_{\dot{q}}$ and τ_δ for system stability under $\Delta_{\hat{M}_\delta^*}$. (For interpretation of the colours in the figure(s), the reader is referred to the web version of this article.)

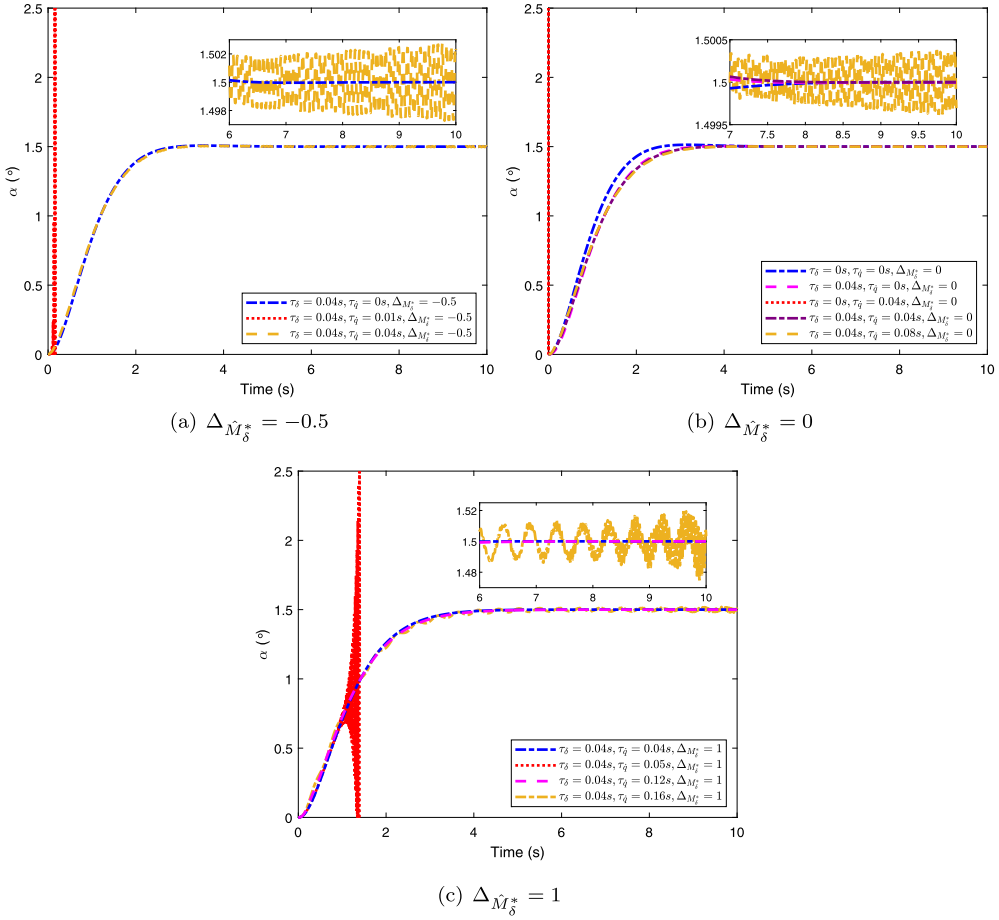

(a) $\Delta_{\hat{M}_\delta^*} = -0.5$ (b) $\Delta_{\hat{M}_\delta^*} = 0$

(c) $\Delta_{\hat{M}_\delta^*} = 1$

Fig. 2. Time response graphs for Aircraft A.

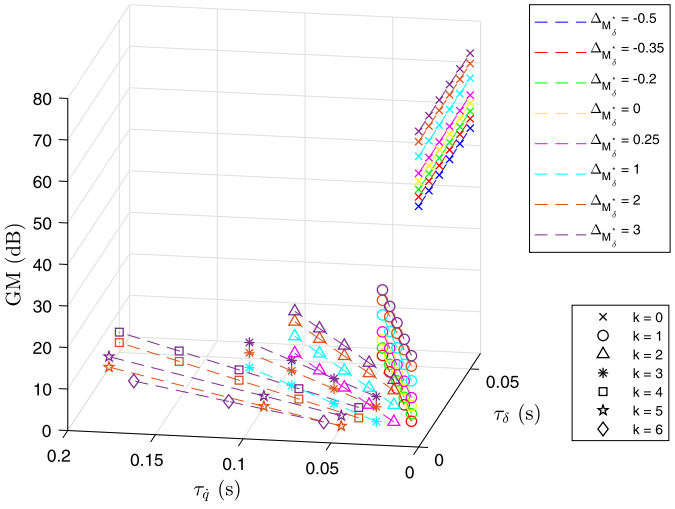

Fig. 3. Gain margin (GM) for stable closed-loop system under $\tau_{\dot{q}}$ and τ_δ together with $\Delta_{\hat{M}_\delta^*}$.

Observation 4.1 and 4.2 can be understood as follows. $\dot{q}_0$ measurement has critical influences on the system with IBKS because it contains the model information about M_α^* and M_q^* to be replaced. If there is no delay on this measurement (i.e. $\tau_{\dot{q}} = 0$ with $k = 0$), the system with IBKS becomes stable. If $\dot{q}_0$ signal is delayed, the relationship between delays on $\dot{q}_0$ and δ_0 becomes important for the system stability due to the following reason. Due to the considered delays on $\dot{q}_0$ and δ_0, trigonometric functions whose frequencies are $\tau_{\dot{q}}$ and τ_δ appear in the characteristic equation (17). The differences between trigonometric terms with frequencies of $\tau_{\dot{q}}$ and τ_δ are repeatedly shown in (17) and they have significant impacts to the closed-loop system stability with IBKS. When $\tau_{\dot{q}} = k\tau_\delta$ with a positive integer k, these differences show a periodic pattern with the frequency of τ_δ like the case without $\tau_{\dot{q}}$, resulting in the stable closed-loop response. k has its upper bound k_{max} determined by the model uncertainty on control effectiveness information $\Delta_{\hat{M}_\delta^*}$, which can be explained as follows. k indicates how many times the cycle of the trigonometric term with $\tau_{\dot{q}}$ is repeated during one period of that with τ_δ. $\Delta_{\hat{M}_\delta^*}$ affects the amplitude of the trigonometric term with $\tau_{\dot{q}}$, as can be seen in (17). The maximum magnitude of the differences between trigonometric terms with frequencies of $\tau_{\dot{q}}$ and τ_δ can be more amplified as k increases, and $\Delta_{\hat{M}_\delta^*}$ has an impact on the magnitude of this amplification. This implies that there exists an upper bound k_{max} which makes the amplification to be within the range where the system is stable and this k_{max} is affected by $\Delta_{\hat{M}_\delta^*}$. The reason why k_{max} decreases as $\Delta_{\hat{M}_\delta^*}$ gets smaller can be explained with loop gain point of view. In the derived control command (14), there exists a reciprocal of $\hat{M}_\delta^*$. This implies that a loop gain becomes smaller with over-estimated $\hat{M}_\delta^*$ (i.e. $\Delta_{\hat{M}_\delta^*} > 0$), while it gets larger with under-estimated $\hat{M}_\delta^*$ (i.e. $\Delta_{\hat{M}_\delta^*} < 0$). Thus, the closed-loop system becomes less robust against the defects as $\Delta_{\hat{M}_\delta^*}$ decreases, resulting in smaller k_{max}. Instead, the time domain response of the system becomes faster as $\Delta_{\hat{M}_\delta^*}$ gets smaller since the loop gain increases.

The comparative study between the closed loop systems with and without measurement delays under model uncertainties is provided as follows. Note that critical understandings about individual and integrated effects of measurement delays and model uncertainties to the system with IBKS can be facilitated by this comparative study. For the closed loop system with model uncertainties and without measurement delays, the previous study in [16] shows that the system with IBKS is not affected by any model uncertainty even in $\hat{M}_\delta^*$ and always stable with uniform performance. When the closed loop system is under both measurement delays and model uncertainties, the relationship between $\tau_{\dot{q}}$ and τ_δ for the system stability is provided, which is affected by $\Delta_{\hat{M}_\delta^*}$. The framework result with $\Delta_{\hat{M}_\delta^*} = 0$ indicates the case when $\tau_{\dot{q}}$ and τ_δ are only considered. In this case, the system is stable only if $\tau_{\dot{q}} = 0$ or $\tau_{\dot{q}} = \tau_\delta$ (i.e. $k_{max} = 1$). If $\Delta_{\hat{M}_\delta^*}$ is additionally considered, the number of stable points tends to decrease with $0 \le k_{max} \le 1$ for under-estimated $\hat{M}_\delta^*$ and increase with $k_{max} \ge 1$ for over-estimated $\hat{M}_\delta^*$.

5. Conclusion

This paper suggests the closed loop characteristics with IBKS under the measurement delays along with the model uncertainties. The analysis framework is proposed to assess absolute stability of the system in a systematic manner by searching unstable poles from the derived characteristic equation with high nonlinearity due to the considered measurement delays. The critical understandings on system stability with IBKS are obtained with the proposed analysis framework as follows. The stability condition is derived as the relationship between the delays on the state derivative and the control surface deflection angle measurements. It is also shown that this condition is affected by the model uncertainty on the control effectiveness information. From the comparative study, the effects of the measurement delays and the model uncertainties to the closed loop system can be understood in individual and integrated manner. The obtained properties from the proposed analysis framework are verified and validated through simulations. Based on the critical insights from the analysis in this paper, further studies with 6 degree-of-freedom dynamics will be conducted as a future work.

Declaration of competing interest

The authors declare that they have no known competing financial interests or personal relationships that could have appeared to influence the work reported in this paper.

Acknowledgement

This research is co-funded by the European Union in the scope of INCEPTION project, which has received funding from the EU's Horizon 2020 Research and Innovation Programme under grant agreement No. 723515.

Appendix A. Derivation of transfer function for the system with IBKS under measurement delays and model uncertainties

Dynamics (2) can be expressed as a state space equation (A.1).

$$\begin{aligned} &\dot{\mathbf{x}} = \mathbf{A}\mathbf{x} + \mathbf{B}\mathbf{u} \qquad \mathbf{y} = \mathbf{C}\mathbf{x} \\ &\mathbf{x} = \begin{bmatrix} \alpha & q \end{bmatrix}^T \qquad \mathbf{u} = \delta \\ &\mathbf{A} = \begin{bmatrix} Z_\alpha^* & 1 \\ M_\alpha^* & M_q^* \end{bmatrix} \quad \mathbf{B} = \begin{bmatrix} 0 \\ M_\delta^* \end{bmatrix} \quad \mathbf{C} = \begin{bmatrix} 1 & 0 \end{bmatrix} \end{aligned} \tag{A.1}$$

Delays on $\dot{q}_0$ and δ_0 measurements are mainly considered for the analysis with IBKS in this paper, and modellings of these delayed measurements are suggested for the closed loop analysis as (A.2) utilizing (2) for $\dot{q}_0$.

$$\begin{aligned} \delta_0 &= \delta\left(t - \tau_\delta\right) \\ \dot{q}_0 &= \dot{q}\left(t - \tau_{\dot{q}}\right) \\ &= M_\alpha^* \alpha\left(t - \tau_{\dot{q}}\right) + M_q^* q\left(t - \tau_{\dot{q}}\right) + M_\delta^* \delta\left(t - \tau_{\dot{q}}\right) \end{aligned} \tag{A.2}$$

Since this paper focuses on IBKS, the model uncertainty $\Delta_{M_\delta^*}$ on $\hat{M}_\delta^*$ is mainly considered in this closed loop analysis. Using (14) with (2), (6) and (A.2) under the assumption of constant α_c (i.e. $\dot{\alpha}_c = \ddot{\alpha}_c = 0$) and zero $\Delta_{Z_\alpha^*}$, δ can be rearranged as (A.3).

$$\begin{aligned} \delta = &-\frac{1}{\hat{M}_\delta^*}\nu_\alpha \alpha - \frac{1}{\hat{M}_\delta^*}\nu_q q + \frac{1}{\hat{M}_\delta^*}\left(C_1 C_2 + 1\right)\alpha_c \\ &- \frac{M_\alpha^*}{\hat{M}_\delta^*}\alpha\left(t - \tau_{\dot{q}}\right) - \frac{M_q^*}{\hat{M}_\delta^*} q\left(t - \tau_{\dot{q}}\right) \\ &+ \left\{\delta\left(t - \tau_\delta\right) - \frac{M_\delta^*}{\hat{M}_\delta^*}\delta\left(t - \tau_{\dot{q}}\right)\right\} \end{aligned} \tag{A.3}$$

where

$$\begin{aligned} \nu_\alpha &= \left\{\left(C_1 + Z_\alpha^*\right)\left(C_2 + Z_\alpha^*\right) + 1\right\} \\ \nu_q &= \left(C_1 + C_2 + Z_\alpha^*\right) \end{aligned}$$

Applying Laplace transform to (A.3) and rearranging the equation with respect to δ,

$$\begin{aligned} \delta(s) = &\left[-\frac{1}{\hat{M}_\delta^* \phi_1(s)}\mu_\alpha(s) \quad -\frac{1}{\hat{M}_\delta^* \phi_1(s)}\mu_q(s) \right]\mathbf{X}(s) \\ &+ \frac{1}{\hat{M}_\delta^* \phi_1(s)}\left(C_1 C_2 + 1\right)\alpha_c(s) \end{aligned} \tag{A.4}$$

where

$$\begin{aligned} \phi_1(s) &= 1 - e^{-\tau_\delta s} + \frac{M_\delta^*}{\hat{M}_\delta^*} e^{-\tau_{\dot{q}} s} \\ \mu_\alpha(s) &= \nu_\alpha + M_\alpha^* e^{-\tau_{\dot{q}} s} \\ \mu_q(s) &= \nu_q + M_q^* e^{-\tau_{\dot{q}} s} \end{aligned}$$

If Laplace transform is applied to (A.1) and $\delta(s)$ in (A.4) is substituted into that equation, the closed loop system can be derived as (A.5).

$$\begin{aligned} &s\mathbf{X}(s) = \mathbf{A}(s)\mathbf{X}(s) + \mathbf{B}(s)\alpha_c(s) \qquad \mathbf{Y} = \mathbf{C}(s)\mathbf{X}(s) \\ &\mathbf{A}(s) = \begin{bmatrix} a_{11}(s) & a_{12}(s) \\ a_{21}(s) & a_{22}(s) \end{bmatrix} \\ &\quad = \begin{bmatrix} Z_\alpha^* & 1 \\ M_\alpha^* - \frac{M_\delta^*}{\hat{M}_\delta^* \phi_1(s)}\mu_\alpha(s) & M_q^* - \frac{M_\delta^*}{\hat{M}_\delta^* \phi_1(s)}\mu_q(s) \end{bmatrix} \\ &\mathbf{B}(s) = \begin{bmatrix} 0 \\ \frac{M_\delta^*}{\hat{M}_\delta^* \phi_1(s)}\left(C_1 C_2 + 1\right) \end{bmatrix} \\ &\mathbf{C}(s) = \begin{bmatrix} 1 & 0 \end{bmatrix} \end{aligned} \tag{A.5}$$

From (A.5), transfer function can be derived as (A.6).

$$\begin{aligned} \frac{\alpha(s)}{\alpha_c(s)} &= \mathbf{C}(s)\left(s\mathbf{I} - \mathbf{A}(s)\right)^{-1}\mathbf{B}(s) \\ &= \frac{a_{12}\frac{M_\delta^*}{\hat{M}_\delta^* \phi_1(s)}\left(C_1 C_2 + 1\right)}{s^2 - \left(a_{11} + a_{22}\right)s + \left(a_{11}a_{22} - a_{12}a_{21}\right)} \end{aligned}$$

$$= \frac{\frac{M_\delta^*}{\hat{M}_\delta^*}(C_1C_2+1)}{\phi_1(s)s^2+\phi_2(s)s+\phi_3}$$

where

$$\phi_1(s) = 1 - e^{-\tau_\delta s} + \frac{M_\delta^*}{\hat{M}_\delta^*}e^{-\tau_{\hat{q}}s} \tag{A.6}$$

$$\phi_2(s) = -(Z_\alpha^* + M_q^*)(1-e^{-\tau_\delta s}) + \frac{M_\delta^*}{\hat{M}_\delta^*}(C_1 + C_2 + Z_\alpha^* - Z_\alpha^* e^{-\tau_{\hat{q}}s})$$

$$\phi_3(s) = (Z_\alpha^* M_q^* - M_\alpha^*)(1-e^{-\tau_\delta s}) + \frac{M_\delta^*}{\hat{M}_\delta^*}(C_1C_2+1)$$

Appendix B. Aerodynamic derivatives

Table B.1
Aerodynamic derivatives of aircraft.

Parameters	Airplane A	Airplane B	Airplane C	Airplane D
h (km)	7.6200	1.5240	1.5240	6.0960
U_0 (m/s)	185.9280	67.0865	103.6320	205.1304
Z_α^*	-1.9626	-0.8222	-2.4660	-0.5249
M_α^*	-4.7488	-17.1690	-23.8147	-1.2473
M_q^*	-3.9326	-6.8791	-5.8557	-0.6474
M_δ^*	-26.6845	-35.2513	-28.4270	-1.6937

References

[1] P.V. Kokotovic, The joy of feedback: nonlinear and adaptive, IEEE Control Syst. Mag. 12 (3) (1992) 7–17.
[2] T. Lee, Y. Kim, Nonlinear adaptive flight control using backstepping and neural networks controller, J. Guid. Control Dyn. 24 (4) (2001) 675–682.
[3] J. Farrell, M. Sharma, M. Polycarpou, Backstepping-based flight control with adaptive function approximation, J. Guid. Control Dyn. 28 (6) (2005) 1089–1102.
[4] H.-S. Ju, C.-C. Tsai, Longitudinal axis flight control law design by adaptive backstepping, IEEE Trans. Aerosp. Electron. Syst. 43 (1) (2007) 311–329.
[5] L.G. Carrillo, A. Dzul, R. Lozano, Hovering quad-rotor control: a comparison of nonlinear controllers using visual feedback, IEEE Trans. Aerosp. Electron. Syst. 48 (4) (2012) 3159–3170.
[6] L. Sonneveldt, Q. Chu, J. Mulder, Nonlinear flight control design using constrained adaptive backstepping, J. Guid. Control Dyn. 30 (2) (2007) 322–336.
[7] B. Lian, H. Bang, Momentum transfer-based attitude control of spacecraft with backstepping, IEEE Trans. Aerosp. Electron. Syst. 42 (2) (2006) 453–463.
[8] Y. Zhang, S.-h. Wang, B. Chang, W.-h. Wu, Adaptive constrained backstepping controller with prescribed performance methodology for carrier-based uav, Aerosp. Sci. Technol. 92 (2019) 55–65.
[9] M. Lungu, Auto-landing of uavs with variable centre of mass using the backstepping and dynamic inversion control, Aerosp. Sci. Technol. (2020) 105912.
[10] M. Lungu, Backstepping and dynamic inversion combined controller for auto-landing of fixed wing uavs, Aerosp. Sci. Technol. 96 (2020) 105526.
[11] P. van Gils, E.-J. Van Kampen, C.C. de Visser, Q.P. Chu, Adaptive incremental backstepping flight control for a high-performance aircraft with uncertainties, in: AIAA Guidance, Navigation, and Control Conference, 2016.
[12] A. Ait Haddou Ali, Q.P. Chu, E.-J. Van Kampen, C.C. de Visser, Exploring adaptive incremental backstepping using immersion and invariance for an f-16 aircraft, in: AIAA Guidance, Navigation, and Control Conference, 2014.
[13] P. Acquatella, E. van Kampen, Q.P. Chu, Incremental backstepping for robust nonlinear flight control, in: Proceedings of the EuroGNC 2013, 2nd CEAS Specialist Conference on Guidance, Navigation and Control, 2013, pp. 1444–1463.
[14] G.P. Falconí, V.A. Marvakov, F. Holzapfel, Fault tolerant control for a hexarotor system using incremental backstepping, in: 2016 IEEE Conference on Control Applications (CCA), IEEE, 2016, pp. 237–242.
[15] B.-J. Jeon, M.-G. Seo, H.-S. Shin, A. Tsourdos, Understandings of the incremental backstepping control through theoretical analysis under the model uncertainties, in: 2018 IEEE Conference on Control Technology and Applications (CCTA), IEEE, 2018, pp. 318–323.
[16] B.-J. Jeon, M.-G. Seo, H.-S. Shin, A. Tsourdos, Understandings of classical and incremental backstepping controllers with model uncertainties, IEEE Trans. Aerosp. Electron. Syst. 56 (4) (2020) 2628–2641.
[17] B.-J. Jeon, M.-G. Seo, H.-S. Shin, A. Tsourdos, Closed-loop analysis with incremental backstepping controller considering measurement bias, IFAC-PapersOnLine 52 (12) (2019) 405–410.
[18] D.I. Ignatyev, H.-S. Shin, A. Tsourdos, Two-layer adaptive augmentation for incremental backstepping flight control of transport aircraft in uncertain conditions, Aerosp. Sci. Technol. (2020) 106051.
[19] L. Cao, X. Li, Y. Hu, M. Liu, J. Li, Discrete-time incremental backstepping controller for unmanned aircrafts subject to actuator constraints, Aerosp. Sci. Technol. 96 (2020) 105530.
[20] S. Sieberling, Q. Chu, J. Mulder, Robust flight control using incremental nonlinear dynamic inversion and angular acceleration prediction, J. Guid. Control Dyn. 33 (6) (2010) 1732–1742.
[21] E.J. Smeur, Q. Chu, G.C. de Croon, Adaptive incremental nonlinear dynamic inversion for attitude control of micro air vehicles, J. Guid. Control Dyn. 38 (12) (2015) 450–461.
[22] F. Grondman, G. Looye, R.O. Kuchar, Q.P. Chu, E.-J. Van Kampen, Design and flight testing of incremental nonlinear dynamic inversion-based control laws for a passenger aircraft, in: 2018 AIAA Guidance, Navigation, and Control Conference, 2018, p. 0385.
[23] P. Acquatella, W. Falkena, E.-J. van Kampen, Q.P. Chu, Robust nonlinear spacecraft attitude control using incremental nonlinear dynamic inversion, in: AIAA Guidance, Navigation, and Control Conference, 2012.
[24] P. Simplício, M. Pavel, E. Van Kampen, Q. Chu, An acceleration measurements-based approach for helicopter nonlinear flight control using incremental nonlinear dynamic inversion, Control Eng. Pract. 21 (8) (2013) 1065–1077.
[25] X. Wang, E.-J. Van Kampen, Q. Chu, P. Lu, Stability analysis for incremental nonlinear dynamic inversion control, J. Guid. Control Dyn. 42 (5) (2019) 1116–1129.
[26] S.H. Lane, R.F. Stengel, Flight control design using non-linear inverse dynamics, Automatica 24 (4) (1988) 471–483.
[27] R. Driver, D. Sasser, M. Slater, The equation x'(t)= ax (t)+ bx (t- τ) with "small" delay, Am. Math. Mon. 80 (9) (1973) 990–995.
[28] S. Guillouzic, I. L'Heureux, A. Longtin, Small delay approximation of stochastic delay differential equations, Phys. Rev. E 59 (4) (1999) 3970.
[29] A. Bahill, A simple adaptive Smith-predictor for controlling time-delay systems: a tutorial, IEEE Control Syst. Mag. 3 (2) (1983) 16–22.
[30] T. Insperger, On the approximation of delayed systems by Taylor series expansion, J. Comput. Nonlinear Dyn. 10 (2) (2015) 024503.
[31] D. McLean, Automatic Flight Control Systems, Prentice Hall, New York, 1990.
[32] C.-H. Lee, B.-E. Jun, J.-I. Lee, Connections between linear and nonlinear missile autopilots via three-loop topology, J. Guid. Control Dyn. (2016) 1426–1432.
[33] M. Powell, A fortran subroutine for solving systems of nonlinear algebraic equations, in: Rabinowitz (Ed.), Numerical Methods for Nonlinear Algebraic Equations, 1970, pp. 115–161.
[34] J. Roskam, Airplane Flight Dynamics and Automatic Flight Controls, DARcorporation, 1998.